Proceedings of 2001 Korea-Japan Joint Seminar
on Particle Image Velocimetry
Seoul National Univ., Dec. 3 - 4

Visualization of Interacting Parallel Supersonic Free Jets using NO-LIF

Tomohide Niimi* and Toshihiko Ishida*

*Department of Electronic-Mechanical Engineering, School of Engineering, Nagoya University, Furo-cho, Chikusa-ku, Nagoya, 464-8603 Japan.

Abstract: The flow field structures of two interacting parallel supersonic free jets are studied by flow visualization using planar laser-induced fluorescence of NO seeded in nitrogen gas. The experiments are carried out for several distances between two orifice centers and for various ratios of the pressure in the reservoir to that in the expansion chamber. The flow fields are visualized mainly on the plane including two jet centerlines and its characteristic shock system, especially a cell structure formed secondly by interaction of two jets, are analyzed. The positions of the normal shock depending on the pressure ratios are also compared.

Keywords: Interacting parallel jets, Second cell, PLIF, Nitric oxide, Shock system

1. Introduction

Recently, investigations on aerospike nozzles expected as a candidate of propulsion engines for the reusable space vehicles have been carried out actively to decrease the loss of propulsion. It is known that the flow field issued from the aerospike nozzle is very similar to two interacting supersonic free jets in a two-dimensional structure on a plane including nozzle centerline(s). In the semiconductor technology, an expansion scheme of reactive gas through multi-orifices into an evacuated chamber has also been suggested to obtain high quality thin films on large scale. To understand these flow field, fundamental knowledge of the flow field of interacting parallel jets is indispensable.

In the present study, therefore, the structures and shock wave systems of two interacting parallel supersonic free jets are investigated by flow visualization using planar laser-induced fluorescence (LIF) of NO seeded in nitrogen gas. The flow fields are visualized mainly on the plane including two jet centerlines. Every flow field shows a symmetrical structure with respect to the geometrical symmetry plane, and has two types of cell surrounded by shock waves; one is formed just downstream of the orifice and the other about the geometrical symmetry plane. The positions of the normal shock depending on the pressure ratios are also compared, changing the distance between the orifice centers as a parameter.

2. Experimental apparatus

Figure 1 illustrates the schematic diagram of the experimental apparatus used for the flow visualization in the present study. A broadband ArF excimer laser (Lambda Physix LPX 105E; wavelength 193 nm, FWHM 0.5nm) is employed as the excitation source. The laser beam has pulse energy of typically 90mJ with 15ns pulse width and excites the $B^2\Pi$-$X^2\Pi$ (7, 0) band (J'' = 23.5-34.5) and the $D^2\Sigma^+$-$X^2\Pi$ (0, 1) band (J'' = 15.5-46.5) of NO near 193 nm. The laser beam propagates to the expansion chamber by three mirrors and then turns into a 0.3-mm-thick and 20-mm-high laser sheet by a fused silica cylindrical lens (400-mm focal length). The beam waist area of the laser sheet is used to visualize the flow field. Nitrogen gas premixed with 1% nitric oxide in a reservoir kept at room temperature expands through two orifices (~ D =

1 mm) into the expansion chamber evacuated by a rotary pump. The flow field in the region of 20 mm × 14 mm is imaged onto a cooled CCD camera set perpendicular to the laser sheet. A BG24 Schott glass (200-nm long pass) filter is mounted to eliminate elastically scattered laser light and to pass most of broadband NO fluorescence. The CCD camera can detect ultra violet fluorescence emitted from nitric oxide molecules with the aid of an image intensifier (Hamamatsu NIGHT VIEWER 2100), although it originally has no sensitivity in a UV region. The steadiness of flow field allows us to accumulate the image data for 3,600 laser shots, and the final images are stored in a personal computer after subtracting dark-current data from the original images. As experimental parameters, we select L/D, a distance between two orifices (L) normalized by a mean orifice diameter (D), and P_s/P_b, a ratio of the pressure in a reservoir (P_s) to the pressure in an expansion chamber (P_b). P_s/P_b is varied over a rage of 74 to 289 and L/D is set at 3, 4, 5, 6 or 7.

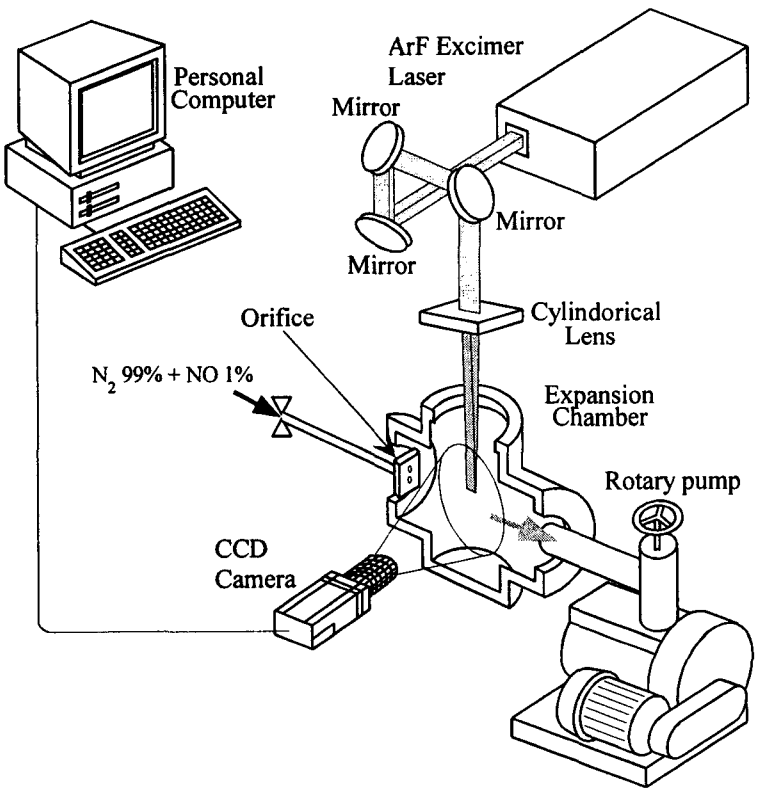

Fig.1 Experimental Apparatus

3. Results and Discussion

3.1 *Characteristic flow field structures of two interacting parallel supersonic free jets*

3.1.1 *Flow field structure for relatively large L/D (L/D = 7)*

Figure 2 provides the visualized image and schematic structure on the plane including two orifice centerlines for L/D = 7 and P_s/P_b = 314. A barrel shock OA formed just downstream of the orifice is reflected on the geometrical symmetry plane, that is, on the plane which bisects the distance between two orifices. The reflected shock turns into the oblique shock AB and terminates in a triple point B with a normal shock BC. From the triple points B and C, reflected shocks BD and CE emanate, respectively. The reflected shock BE terminates in another triple point D with a normal shock DD′ and reflected shock DF, showing a complicated shock system. As can be seen in the photograph, slip lines emanate from the triple points B and C because of discontinuity of the velocity. There appears a cell surrounded by oblique shocks

about the symmetry plane, which we call 'the second cell' in contrast to 'the first cell' formed just downstream of the orifice.

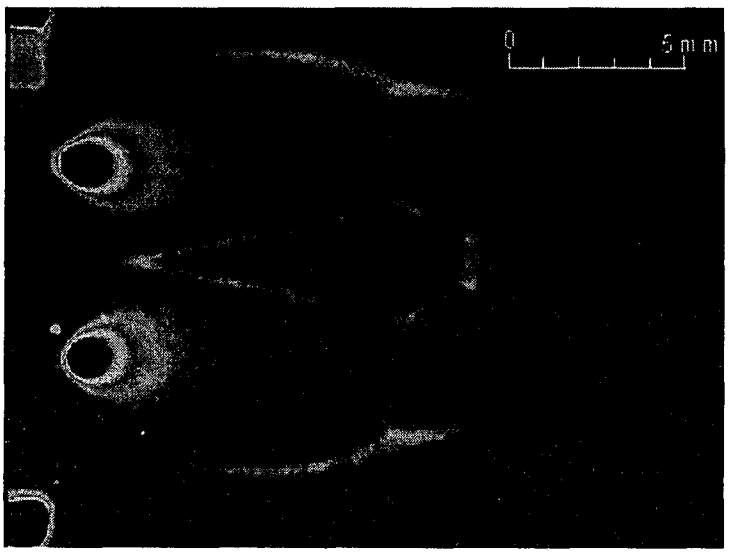

(a)

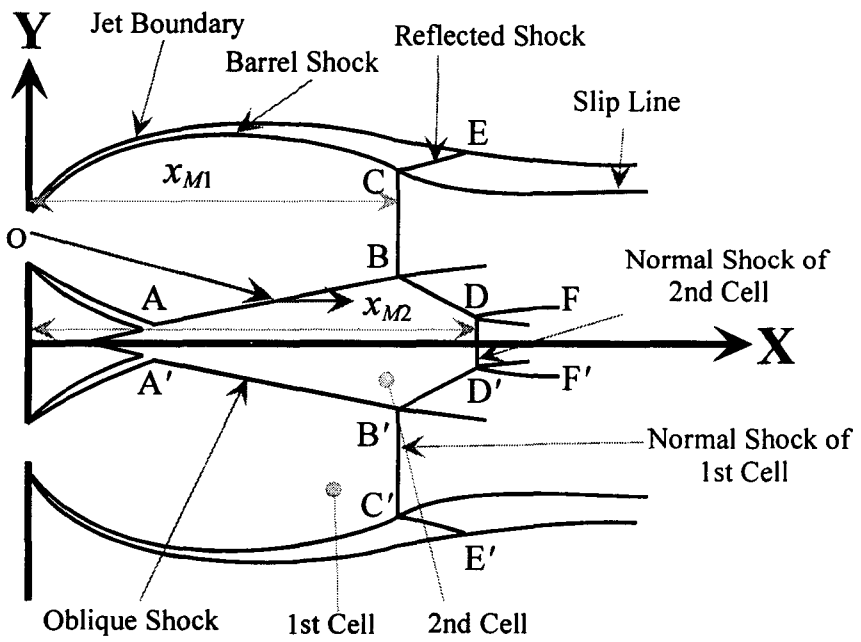

(b)

Fig.2 The flow field structure for L/D = 7 and P_s/P_b = 314; (a) flow visualization and (b) schematic structure of the flow field.

3.1.2 *Flow field structure for relatively small L/D (L/D = 3)*

For relatively small L/D, the flow field of two interacting parallel supersonic free jets with the similar pressure ratio as that for Fig. 2 results in the image and structure as shown in Fig. 3. The oblique shock AB intersects with the barrel shock OB at the point B, showing no normal shock in the first cell. The reflected shocks BC and BD also emanate from the point B.

In general, the flow in a single jet is approximated as a point source flow and then its streamlines are depicted by the lines radiated from the point source. Compared the terminal point B of the oblique shock in Fig. 3 with that in Fig. 2, the point B in Fig. 3 exists above the centerline of the upper jet while the point B in Fig. 2 below that. The streamline near the point B in Fig. 3 proceeds in the opposite direction to the symmetry plane after passing through the oblique shock, but that in Fig. 2 in the parallel direction to the plane. This means that the flow field inside the second cell in Fig. 3 expands more strongly than that in Fig. 2. The stronger expansion may be attributed to that density at the starting point of interaction AA′ becomes higher as L/D decreases. This may be the reason why there appears no normal shock in the first cell in Fig. 3. Apart from the oblique shocks, the flow field structure of two interacting supersonic free jets for the lower value of L/D is very similar to that of a single supersonic free jet.

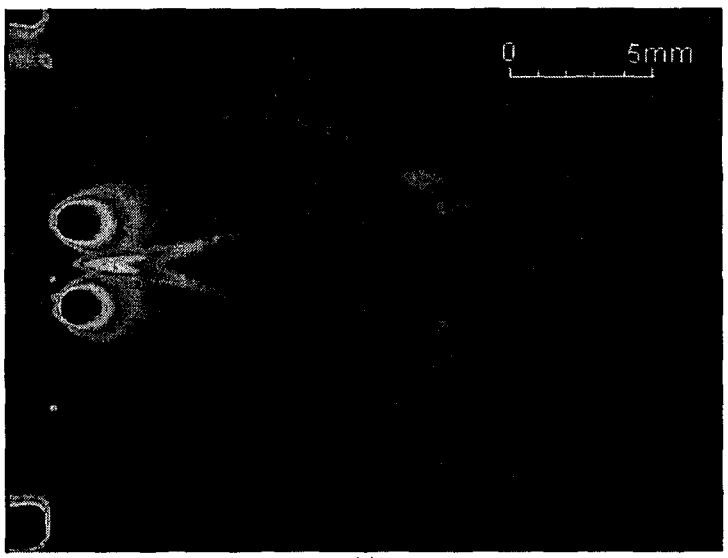

(a)

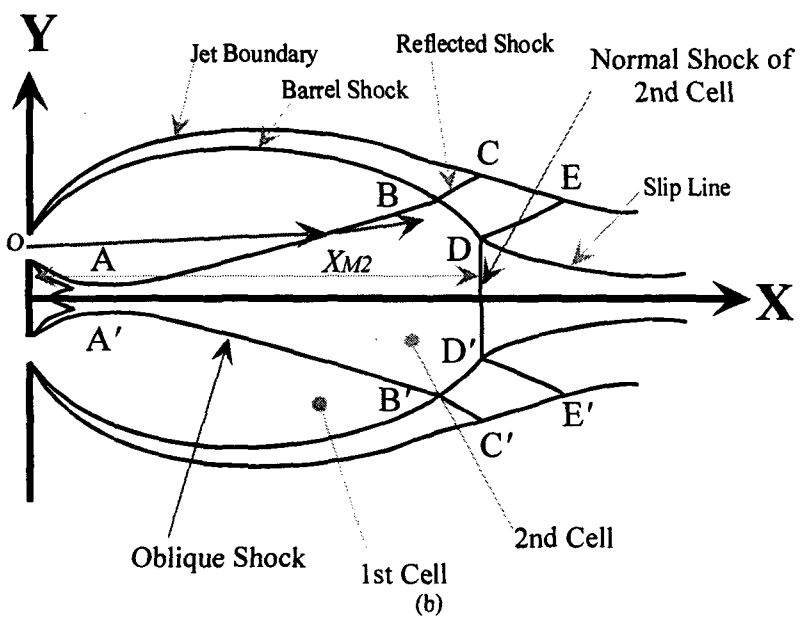

(b)

Fig.3 The flow field structure for $L/D = 3$ and $P_s/P_b = 289$; (a) flow visualization and (b) schematic structure of the flow field

3.2 *Transition of the flow field structure with pressure ratios*

Figures 4 and 5 show the transition of the flow field structure depending on P_s/P_b for L/D = 7 and 3, respectively. For L/D = 7, the two jets grow self-similarly and then start to interact each other as P_s/P_b increases (see Fig. 4(a)). For P_s/P_b = 189, the reflected shocks intersect at a brighter point on the symmetry plane and the second cell without a normal shock is formed. As P_s/P_b increases further, the normal shock appears in the second cell due to an increase in the Mach number inside the second cell, as shown in Fig. 2 (a). For L/D =3, we find the second cell and then the normal shock in the second cell even at the lowest pressure ratio in this study. As an increase in P_s/P_b, the flow field grows self-similarly, remaining the similar flow field structure.

(a) P_s/P_b = 144

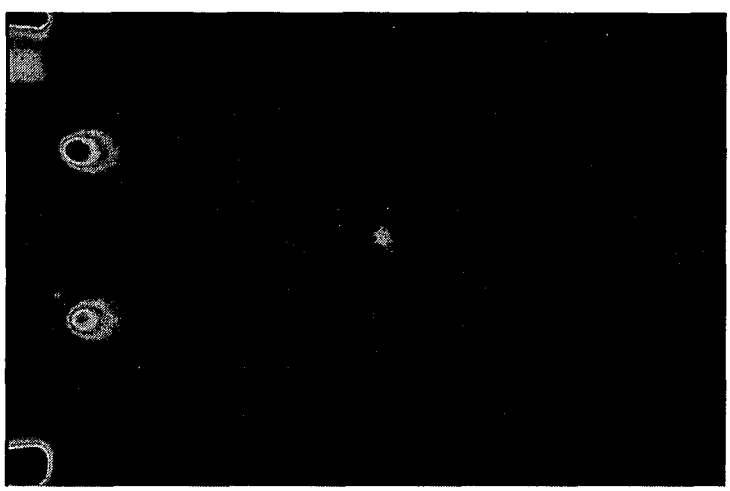

(b) P_s/P_b = 189

Fig.4 Transition of the flow field structure with pressure ratios for L/D = 7

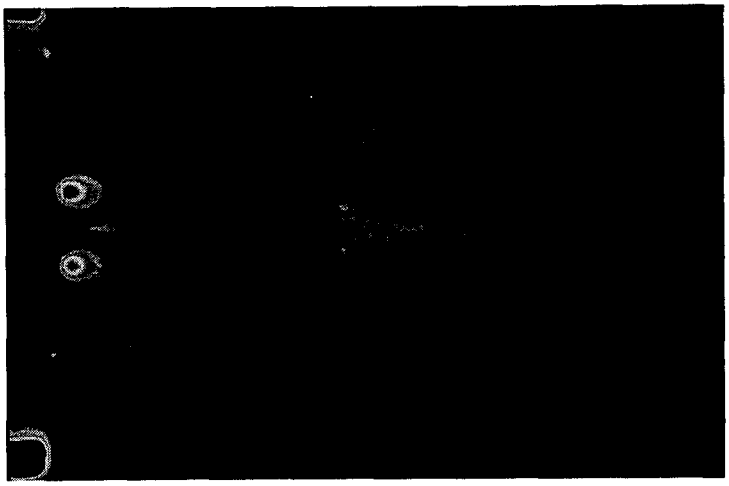

(a) $P_s/P_b = 146$

(b) $P_s/P_b = 189$

Fig.5 Transition of the flow field structure with pressure ratios for $L/D = 3$

3.3 *The position of the normal shock*

To examine the flow fields of two interacting supersonic free jets quantitatively, the distances of the normal shock from the orifice wall in the first cell (x_{M1}) and the second cell (x_{M2}) are measured on P_s/P_b for each L/D, as shown in Fig. 6 and 7, respectively. The distance x_{M1} and x_{M2} are normalized by the mean orifice diameter D in these figures. The solid curve in Fig. 6 indicates x_{M1} for a single supersonic free jet, given empirically by Ashkenas and Sherman (Ashkenas and Sherman, 1984). It is evident from Fig. 6 that the normal shock in the first cell moves downstream as P_s/P_b increases. The values of x_{M1}/D for $L/D = 6$ and 7 agree with those for the single supersonic free jet irrespective of P_s/P_b in the range of our experiments, whereas the values of x_{M1}/D for $L/D = 5$ are deviated to the upper side from the solid curve, indicating that the normal shock is formed more downstream than for the single supersonic free jet.

The distance of the normal shock in the second cell hardly depends on the values of L/D, as shown in Fig. 7, although the change of L/D has a significant influence on the structure of the flow field as mentioned in 3.2. Since the starting point of interaction shifts upstream as a decrease in L/D, the pressure at that position increases and then the normal shock in the second cell moves downstream. This may be the reason why the distance of the normal shock in the second cell remains nearly constant irrespective of L/D. The

solid curve in Fig. 7 is approximated as follows by a method of least squares for the experimental data.

$$\frac{x_{M2}}{D} = 0.71\left(\frac{P_s}{P_b}\right)^{0.531} \tag{1}$$

The date calculated by Usami and Teshima (Usami and Teshima, 1999) using the DSMC method are also included in Fig. 7, which agree well with the approximated curve as can be seen.

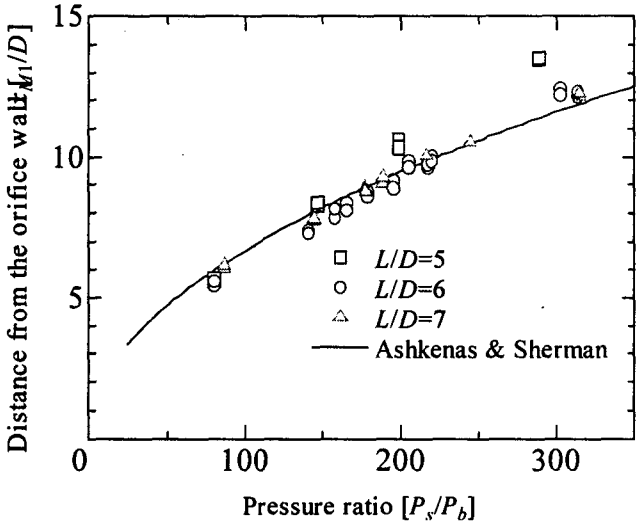

Fig.6 The position of the normal shock in the first cell

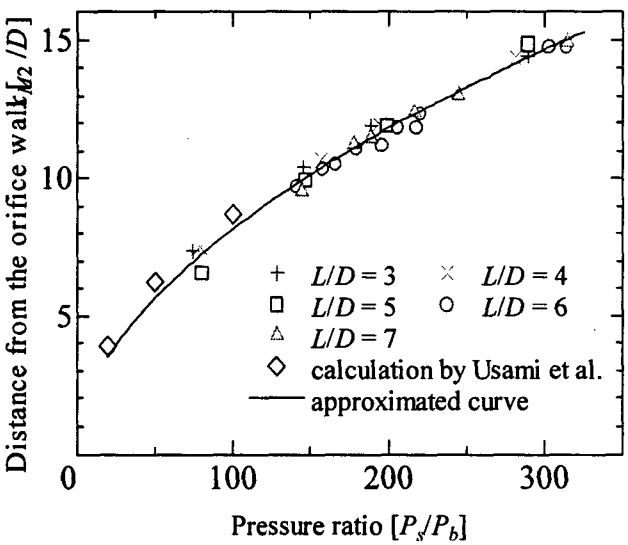

Fig.7 The position of the normal shock in the second cell

4. Conclusion

In the present study, the flow field structures of two interacting parallel supersonic free jets are visualized using the NO-LIF method. It is found that there appears the second cell surrounded by oblique shocks about the geometrical symmetry plane, also showing the complicated shock system with respect to *L/D*.

The distance of the normal shock in the first cell depends both on L/D and P_s/P_b, while the distance of the normal shock in the second cell depends hardly on L/D.

References

Ashkenas, H. and Sherman, F. S., 1966, "The Structure and Utilization of Supersonic Free Jets in Low Density Wind Tunnels", Proc. of 4th Int. Symp. Rarefied Gas Dynamics, Oxford, England, Vol.2, 84.

Usami, M. and Teshima, K., 1999, "Three Dimensional DSMC Calculation for Plume-Plume Interaction of Parallel Supersonic Jets", Trans. Jpn. Soc. Mech. Eng., (B), Vol.65, No.630, 444.